RESEARCH ARTICLE

Mathematical Modeling of an Integrated Microbial Fuel Cell-Bioreactor System for Slaughterhouse Wastewater Treatment

D. Gowthaman[1], A. Shamadhani Begum[2], S. Thamizh Suganya[1], Muhammad Rafiq[3] and Muhammad Ijaz Khan[4,*]

[1] Department of Mathematics, AMET Deemed to be University, Chennai 603112, India
[2] Department of Science and Humanities, Sri Krishna College of Engineering and Technology, Coimbatore 641008, India
[3] College of Business Administration, Prince Mohammad Bin Fahd University, Al Khobar 31952, Saudi Arabia
[4] Department of Mechanical Engineering, Prince Mohammad Bin Fahd University, Al Khobar 31952, Saudi Arabia

Abstract

This study presents an analytical mathematical model for an integrated microbial fuel cell–oxic–anoxic bioreactor (MFC–OB–ANB) system designed for simultaneous slaughterhouse wastewater treatment and energy recovery. The model incorporates bioelectrochemical oxidation, nitrification, and denitrification processes using acetate as a representative substrate. Closed-form analytical solutions are derived for substrate degradation, nitrogen transformation, current density, and system voltage. The effects of biofilm thickness, membrane conductivity, and influent substrate concentration on treatment efficiency and power generation are systematically investigated. Results reveal that enhanced biofilm conductivity and reduced membrane resistance significantly improve energy recovery, while optimized substrate loading enhances nitrogen removal performance. The proposed framework provides valuable insights for the design and optimization of integrated bioelectrochemical wastewater treatment systems.

Keywords: microbial fuel cell, mathematical model, Nernst-Monod model, slaughterhouse wastewater, new homotopy perturbation method, nonlinear equations, nitrification and de-nitrification model.

1 Introduction

A major global environmental issue involves water source pollution from organic material. Stringent environmental regulations have sped up the creation of technologies for treatment of wastewater since these technologies aim at extracting valuable goods as well as resources while also achieving pollution control's objective [1, 2]. For sustainable sources [3] of energy recovery substrates comes the bio electrochemical device (BES) development from organic-rich agro-industrial waste. Many suspended solids and liquid waste and odours are

Submitted: 24 November 2025
Accepted: 18 December 2025
Published: 28 December 2025

Vol. 1, **No.** 2, 2025.
10.62762/IJTSSE.2025.805399

***Corresponding author:**
✉ Muhammad Ijaz Khan
mkhan1@pmu.edu.sa

Citation
Gowthaman, D., Begum, A. S., Suganya, S. T., Rafiq, M., & Khan, M. I. (2025). Mathematical Modeling of an Integrated Microbial Fuel Cell-Bioreactor System for Slaughterhouse Wastewater Treatment. *International Journal of Thermo-Fluid Systems and Sustainable Energy*, 1(2), 96–107.

Table 1. Technology implemented for abattoir wastewater.

S.No	Technology implemented	Source properties for abattoir wastewater.	References
1	Anaerobic digestion of slaughterhouse effluent using a UASB reactor and anaerobic filter (AF).	COD: 8000mg/L, Proteins: 70%, Detached solid information: among 15 and 30% of the COD.	Ruiz et al. [8]
2	Fixed bed sequencing batch reactor (FBSBR).	COD range: 0.5 -1.5 Kg COD/m3 per day.	Rahimi et al. [9]
3	A hybrid upflow anaerobic sludge blanket (HUASB) reactor can treat effluent from chicken slaughterhouses.	COD: 3000-4800 mg/L, resolvable COD: 1030 - 3000mg/L, BOD5: 750 -1890 mg/L, deferred solids:300 - 950mg/L, alkalinity (as CaCO3): 600 - 1340mg/L, VFA (as acetate): 250 - 540mg/L pH: 7 - 7.6.	Rajakumar et al. [10]
4	The anaerobic hybrid reactor was stocked with ultralight floating medium.	COD: 22000 - 27500mg/L, BOD:10800 - 14600mg/L, Deferred Solids: 1280 - 1500mg/L.	Sunder and Satyanarayan [11]

the primary environmental issue associated with this slaughterhouse wastewater [4].

Surface and groundwater, effluent from slaughterhouses has also been recognized that blood, fat, manure, and urine are lost to the wastewater streams during slaughterhouse [5]. Groundwater leaching is a major concern of the recalcitrant presence of such pollutants [6]. Blood has the highest COD of effluent from abattoir activities a key dissolved contaminant in wastewater. The effluent load would be equal to the total amount of sewage that is generated on an average day by 50 [7]. This would result from blood discharge from one cow carcass flowing straight into the sewer line.

The meat processing industry consumes 29% of total freshwater utilized by the agriculture sector globally [12, 13], which has risen over the last decade and is anticipated to continue to rise until 2050. The number of slaughterhouse facilities is growing, resulting in an anticipated higher amount of wastewater from slaughterhouses (SWW) to be treated [14]. Due to its efficacy for handling high-strength wastewater like SWW, anaerobic treatment favours biological treatment with less complicated equipment [15]. Biological processes alone cannot yield effluent that complies with discharge limits for wastewater with high organic intensity. For the future recovery of resources and for the high quality of treatment, the use of mixed anaerobic and aerobic processes is helpful as well [16].

An MFC may use complex organic substrates as a source for power generation as it can include residential industrial as well as agricultural wastewater. This attracts attention since the MFC is a promising technology; it links renewable energy and waste treatment [17, 18]. Several researchers have successfully employed various slaughterhouse wastewater treatment systems incorporating organic carbon and nitrogen (COD and TKN) in laboratory and pilot studies. The mathematical modeling of microbial fuel cells in wastewater treatment employs a novel homotopy perturbation approach [19]. A summary of conventional technologies previously implemented for abattoir wastewater treatment is presented in Table 1.

Slaughterhouse wastewater is a high-strength effluent that poses severe environmental risks due to its high concentrations of organic matter, ammonium, suspended solids, and pathogenic microorganisms [20]. Conventional treatment methods such as activated sludge or anaerobic digestion often fail to meet discharge standards due to limitations in nitrogen removal and energy recovery. Integrating microbial fuel cells (MFCs) with oxic and anoxic bioreactors provides a hybrid solution capable of simultaneous organic degradation, nitrification, denitrification, and bioelectricity generation. The MFC reduces the organic load while producing electricity; the oxic bioreactor enables ammonium oxidation, and the anoxic bioreactor ensures complete nitrogen removal through denitrification. This integrated configuration addresses the challenges of treating slaughterhouse wastewater more effectively than conventional standalone systems [21, 22]. The schematic diagram of the proposed integrated MFC–OB–ANB system is illustrated in Figure 1.

Table 2. Nomenclature Table (Part 1).

Symbol	Description (Units)
S_{AC}	Acetate content during any given time. (mg/L)
X	The concentration of biomass, (mg/L)
S_{H^+}	The concentration of hydrogen ions at any given time (mg/L)
S_{CO_2}	Carbon dioxide amounts at any given period. (mg/L)
$S_{NH_4^+}$	Ammonium levels amounts at any given period, (mg/L)
S_{O_2}	The concentration of dissolved oxygen at any given time (mg/L)
$S_{NO_3^-}$	Nitrate levels at any moment. (mg/L)
S_{OH^-}	Hydroxyl ion level at any given period, (mg/L)
S_M	The concentration of activities in the cathode chamber at any one moment (mg/L)
S_{N_2}	Nitrogen absorption at any given period, (mg/L)
j	Current density, (mA/cm^2)
η	Spatial loss possibilities can be described as $\eta = E_{an} - E_{KA}$
E_{KA}	Halfway or midway potential, $(volt)$
S_{AC}^{in}	Inflowing acetate concentration, (mg/L)
X^{in}	Biomass concentration in the incoming stream, (mg/L)
$S_{H^+}^{in}$	Hydrogen ion concentration in the inflow, $((mg/L)$
$S_{CO_2}^{in}$	Carbon dioxide level in the influent, (mg/L)
$S_{NH_4^+}^{in}$	Ammonium concentration in the feed stream, (mg/L)
$S_{O_2}^{in}$	Dissolved oxygen level in the influent, (mg/L)
$S_{NO_3^-}^{in}$	Nitrate concentration in the incoming solution, (mg/L)
S_{OH}^{in}	Hydroxyl ion level in the incoming stream, (mg/L)
S_M^{in}	Cation concentration entering the cathode chamber, (mg/L)
S_{N_2}	Nitrogen concentration in the feed at a given time, (mg/L) (mg/L)
V_a	Total volume of the anode compartment, (m^3)
V_c	Cathode chamber volume, (m^3)
Q_a	Inflow rate to the anode chamber, (L/day)
Q_c	Inflow rate to the cathode chamber, (L/day)
A_m	Area of the membrane surface perpendicular to flow, (m^2)
$r_{ut,an}$	Substrate consumption rate per unit electrode area, $(mg/cm^2.day)$
$r_{nit,cat}$	Surface-based nitrification rate in the cathode compartment
$r_{res,cat}$	Reaction rate of endogenous respiration in the cathode compartment, $(mg - VS/cm^2.day)$
r_{nit}	Nitrification process rate, $(mg - N/cm^2.day)$
r_{dn}	Rate of denitrification, $(mg - N/cm^2.day)$
$b_{res,an}$	Reaction constant for endogenous respiration in the cathode chamber, (L/day)
q_{an}	Electron donor utilization rate per unit biomass, $(mmol - ED/mg - VS.day)$
$q_{max,an}$	Peak electron donor utilization rate per unit biomass, $(mmol - ED/mg - VS.day)$
q_{max,NH_4^+}	Peak specific ammonium consumption rate, $(mg - N/mgVS.day)$
q_{max,NO_3^-}	Maximum rate of nitrate reduction per unit biomass, $(mg - N/mgVS.day)$

2 SYSTEM BOUNDARY AND ASSUMPTIONS

The model simulates a continuous-flow integrated MFC-OB-ANB system for slaughterhouse wastewater treatment. The system boundary includes:

- **Influent:** High-strength slaughterhouse wastewater containing acetate (as representative COD), ammonium, and nitrate.
- **Reactor Units:** (i) MFC unit for partial COD removal and current generation, (ii) Oxic Bioreactor (OB) for nitrification, and (iii) Anoxic Bioreactor (ANB) for denitrification.
- **Effluent:** Treated water with reduced COD, ammonium, and nitrate.

Interactions between units include flow continuity,

Table 3. Nomenclature Table (Part 2).

Symbol	Description (Units)
S_d	Level of ED in the system, $(mmol - ED/cm^3)$
$K_{S,d}$	ED level corresponding to 50% of the maximum utilization rate $(mmol - ED/cm^3)$
S_a	Electron acceptor concentration (EA), $(mmol - EA/cm^3)$
$K_{S,a}$	EA concentration at half-maximal utilization rate $(mmol - EA/cm^3)$
$\varnothing_{E,a}$	Dimensionless proportion of active electrogenic microorganisms $(dimensionless)$
$S_a^{\hat{A}^\circ}$	Reference concentration of the anodic electron acceptor $(1mmol - EA/cm^3)$
$f_e^{\hat{A}^\circ}$	Proportion of electron donor used for energy generation
$E_{an}^{\hat{A}^\circ}$	Standard electrode potential of the anodic electron acceptor, $(volt)$
R	Universal gas constant, $(8.3145 J/mol.K)$
F	Charge per mole of electrons/Faraday constant, $(96485 Coulomb/mole.e^-)$
T	System temperature, $(298.15K)$
n	Moles of electrons exchanged per mole of anodic EA
X_F	Density of metabolically active microorganisms $(mg - VS/cm^3)$
P	Power, (mW)
I	Current, (mA)
R_{ext}	Resistance, (ohm)
E_{cell}	Cell voltage, $(volt)$
L_f	Bio film thickness, (cm)
j_{an}	Current generated per unit area of the anode (mA/cm^2)
$j_{\max}$	Maximum achievable current per unit electrode area, (mA/cm^2)
N	Positive ion flux across the membrane from anode to cathode
f_x	Inverse of the washout rate
Y_{AC}	Microbial growth yield using acetate as the substrate $(mg\ acetate/mg\ NO_3 - N)$
$Y_{NH_4^+}$	Microbial growth efficiency on NH_4^+ substrate, $(mg\ VS/mg\ NH_4^+ - N)$
K_{N,NH_3}	Substrate concentration at half-maximal uptake rate for autotrophs, $(molNH_4^+/L)$
$K_{N,O}$	Dissolved oxygen level at half-maximal rate for autotrophs, $(mol\ O_2/L)$
S_0	Oxygen level in the system $(mol\ DO/L)$
X_n	Level of active nitrifying microorganisms, (mg/L)
V_{nb}	Nitrification reactor volume, (L)
V_{dn}	Total volume of the denitrification bioreactor under anoxic conditions, (L)
X_{dn}	Level of active denitrifying microorganisms, $(mg\ VS/m^3)$
K_{d,NO_3^-}	Nitrate concentration at half-maximal microbial uptake rate, (mg/L)
$K_{d,AC}$	Acetate concentration at half the maximum utilization rate, (mg/L)
$\alpha_{AC,1}, \alpha_{AC,2}$	Dimensionless acetate conversion in MFC and denitrification processes
$\alpha_{NH_4^+,1}, \alpha_{NH_4^+,2}$	Dimensionless ammonium conversion in MFC and nitrification processes
k_{bio}	Biofilm electrical conductivity, (mS/cm)
ρ_f	Mass of biofilm per unit area, (g/m^3)
f_a	Active biomass volume ratio (dimensionless)
d^m	Physical thickness of the membrane layer, (m)
d_{cell}	Separation between anode and cathode, (m)
k^m	Membrane electrical conductivity, $(1/ohm.m)$
k^{aq}	Electrical conductivity of the bulk solution, $(1/ohm.m)$
M	Molecular weight of oxygen (O_2)
b	Electron transfer number per mole of O_2
$\in_{cb}$	Efficiency of electron recovery as electrical current
γ_s	Mass-to-charge conversion factor
E_{an}^o	Reference electrode potential for the anodic EA, $(volt)$

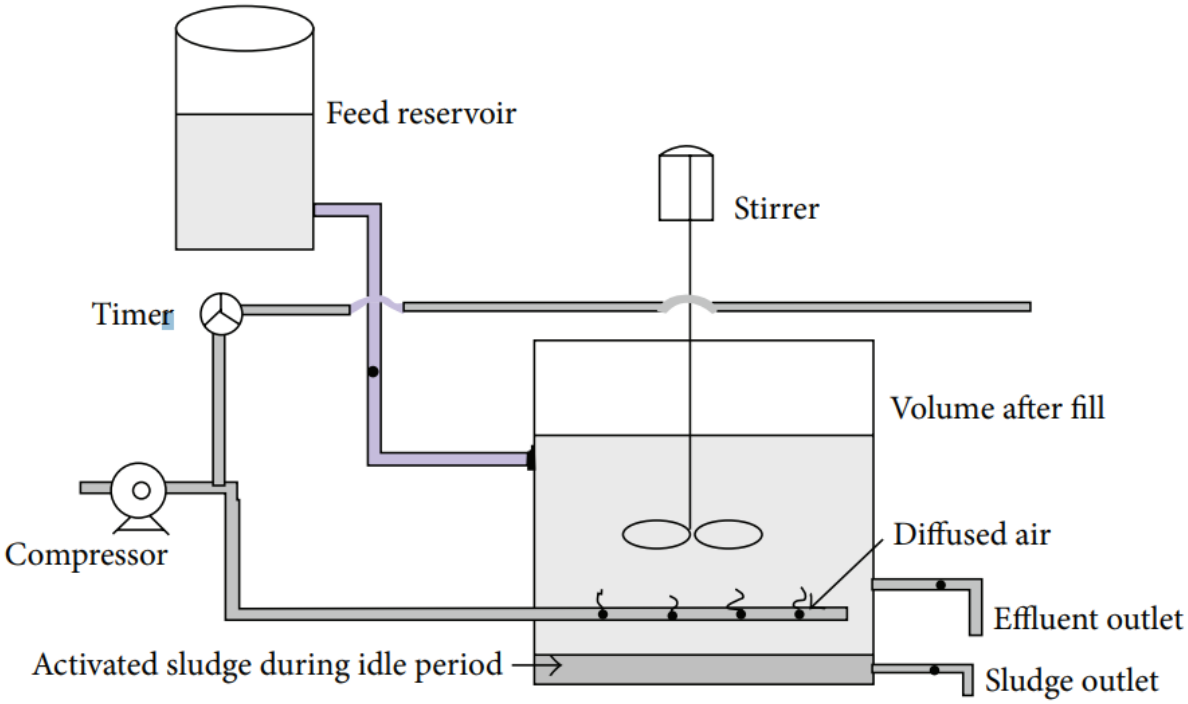

Figure 1. Schematic of the integrated MFC-OB-ANB system. The system includes an MFC unit for organic degradation and power generation, followed by an Oxic Bioreactor (OB) for nitrification and an Anoxic Bioreactor (ANB) for denitrification. Arrows indicate wastewater flow direction.

Table 4. Parameter values.

Parameter	Symbol	Value	Unit	Source
Biofilm thickness	δ	20	μm	Assumed
Membrane conductivity	σ_m	0.1	S/m	Literature [21]
Influent COD (Acetate)	S_{in}	12000	mg/L	Measured
NH_4^+ concentration	N_{in}	500	mg/L	Measured
Temperature	T	298	K	Assumed
DO half-saturation	K_O	0.2	mg/L	Literature [22]

substrate transformations, and electron transfers. The model assumes steady-state operation with uniform flow and ideal mixing in bioreactors.

3 Model description

The nomenclature and symbols used throughout the mathematical model are listed in Tables 2 and 3 for reference. The Nernst-Monod equation and the growth rate of Nernst-related bacteria are used to calculate the potential for electrodes [21, 22]. The Anodic reaction are

$$2HCO_3^- + 9H^+ + 8e^- \rightarrow CH_3COO^- + 4H_2O \quad (1)$$

The Cathode reaction:

$$\frac{3}{2}O_2 + 6H^+ + 6e^- \rightarrow 3H_2O \quad (2)$$

$$NH_4^+ + 2H_2O \rightarrow NO_2^- + 8H^+ + 6e^- \quad (3)$$

$$2NH_4^+ + 3O_2 \xrightarrow{AOB} 2NO_2^- + 4H^+ + 2H_2O \quad (4)$$

The ultimate metabolic process by nitrobacteria (NOB) creates nitrate as follows:

$$NO_2^- + 1/2O_2 \xrightarrow{NOB} NO_3^- \quad (5)$$

The mass distribution of the microbial fuel cell (MFC):

$$V_a \frac{dS_{AC}}{dt} = Q_a \left(S_{AC}^{in} - S_{AC}\right) - A_m r_{ut,an} \quad (6)$$

$$V_a \frac{dX}{dt} = Q_a \left(\frac{X^{in} - X}{f_X}\right) + A_m Y_{ac} r_{ut,an} - V_a b_{res,an} X \quad (7)$$

$$V_a \frac{dS_{H^+}}{dt} = Q_a \left(S_{H^+}^{in} - S_{H^+}\right) + 8A_m r_{ut,an} \quad (8)$$

$$V_a \frac{dS_{CO_2}}{dt} = Q_a \left(S_{CO_2}^{in} - S_{CO_2}\right) + 2A_m r_{ut,an} \quad (9)$$

$$V_a \frac{dS_{NH_4^+}}{dt} = Q_a \left(S_{NH_4^+}^{in} - S_{NH_4^+}\right) - N_{NH_4^+ - N} A_m \quad (10)$$

where

$$r_{ut,an} = q_{\max,m} X_F \varnothing_{E,a} \left(\frac{S_{AC}}{S_{AC} - K_{S,AC}}\right) \left[\frac{1}{1+\exp\left(-\frac{F}{RT}\eta\right)}\right] \tag{11}$$

The analytical solution of mass balance for the microbial fuel cell:

$$S_{AC}(t) = S^*_{AC} e^{-\frac{Q_a}{V_a}t} + \left(S^{in}_{AC} - \frac{A_m q_{\max,m} X_F \varnothing_{E,a}}{Q_a}\left(\frac{S^*_{AC}}{S^*_{AC} - K_{S,AC}}\right) \left[\frac{1}{1+\exp\left(-\frac{F}{RT}\eta\right)}\right]\right)\left(1 - e^{-\frac{Q_a}{V_a}t}\right) \tag{12}$$

$$X(t) = X^* e^{-\frac{Q_a}{V_a f_X}t} - \left(\frac{b_{res,am} V_a f_X}{Q_a} - X^{in}\right)\left(1 - e^{-\frac{Q_a}{V_a f_X}t}\right) + \frac{A_m Y_{ac} f_X q_{\max,m} X_F \varnothing_{E,a}}{Q_a}\left(\frac{S^*_{AC}}{S^*_{AC} - K_{S,AC}}\right) \left[\frac{1}{1+\exp\left(-\frac{F}{RT}\eta\right)}\right]\left(1 - e^{-\frac{Q_a}{V_a f_X}t}\right) \tag{13}$$

$$S_{H^+}(t) = S^*_{H^+} e^{-\frac{Q_a}{V_a}t} + \left(S^{in}_{H^+} + \frac{8 A_m q_{\max,m} X_F \varnothing_{E,a}}{Q_a}\left(\frac{S^*_{AC}}{S^*_{AC} - K_{S,AC}}\right) \left[\frac{1}{1+\exp\left(-\frac{F}{RT}\eta\right)}\right]\right)\left(1 - e^{-\frac{Q_a}{V_a}t}\right) \tag{14}$$

$$S_{CO_2}(t) = S^*_{CO_2} e^{-\frac{Q_a}{V_a}t} + \left(S^{in}_{CO_2} + \frac{2 A_m q_{\max,m} X_F \varnothing_{E,a}}{Q_a}\left(\frac{S^*_{AC}}{S^*_{AC} - K_{S,AC}}\right) \left[\frac{1}{1+\exp\left(-\frac{F}{RT}\eta\right)}\right]\right)\left(1 - e^{-\frac{Q_a}{V_a}t}\right) \tag{15}$$

$$S_{NH_4^+}(t) = S^*_{NH_4^+} e^{-\frac{Q_a}{V_a}t} + \left(S^{in}_{NH_4^+} - \frac{N_{NH_4^+ - N} A_m}{Q_a}\right)\left(1 - e^{-\frac{Q_a}{V_a}t}\right) \tag{16}$$

In the cathode cavity, the mass equilibrium of liquefied oxygen (DO), NH_4^+, NO_3^-, OH^- and cations M^+ are stated as follows

$$V_c \frac{dS_{O_2}}{dt} = Q_c\left(S^{in}_{O_2} - S_{O_2}\right) + A_m r_{nit,cat} \tag{17}$$

$$V_c \frac{dX}{dt} = Q_c\left(\frac{X^{in} - X}{f_X}\right) + A_m Y_{NH_4^+} r_{nit,cat} - V_c b_{\text{res},cat} X \tag{18}$$

$$V_c \frac{dS_{NH_4^+}}{dt} = Q_c\left(S^{in}_{NH_4^+} - S_{NH_4^+}\right) + A_m r_{nit,cat} \tag{19}$$

$$V_c \frac{dS_{NO_3^-}}{dt} = Q_c\left(S^{in}_{NO_3^-} - S_{NO_3^-}\right) - A_m r_{nit,cat} \tag{20}$$

$$V_c \frac{dS_{OH^-}}{dt} = Q_c\left(S^{in}_{OH^-} - S_{OH^-}\right) - 4 A_m r_{nit,cat} \tag{21}$$

$$V_c \frac{dS_M}{dt} = Q_c\left(S^{in}_M - S_M\right) + N A_m \tag{22}$$

Where

$$r_{nit,cat} = -q_{\max,cat} X_f L_f \left(\frac{S_{NH_4^+}}{S_{NH_4^+} - K_{S,NH_4^+}}\right)\left[\frac{1}{1+\exp\left(-\frac{F}{RT}\eta\right)}\right] \tag{23}$$

The analytical solution of mass balance for the microbial fuel cell:

$$S_{O_2}(t) = S^*_{O_2} e^{\frac{Q_c}{V_c}t} + \left(S^{in}_{O_2} + \frac{A_m q_{\max,cat} X_f L_f}{Q_c}\left(\frac{S_{NH_4^+}}{S_{NH_4^+} - K_{S,NH_4^+}}\right) \left[\frac{1}{1+\exp\left(-\frac{F}{RT}\eta\right)}\right]\right)\left(1 - e^{\frac{Q_c}{V_c}t}\right) \tag{24}$$

$$X(t) = X^* e^{\frac{Q_c}{V_c f_X}t} - \left(\frac{b_{\text{res},cat} V_c f_X}{Q_c} - X^{in} - \frac{A_m Y_{NH_4^+} q_{\max,cat} X_f L_f}{Q_c}\left(\frac{S_{NH_4^+}}{S_{NH_4^+} - K_{S,NH_4^+}}\right) \left[\frac{1}{1+\exp\left(-\frac{F}{RT}\eta\right)}\right]\right)\left(1 - e^{\frac{Q_c}{V_c f_X}t}\right) \tag{25}$$

$$S_{NH_4^+}(t) = S^*_{NH_4^+} e^{\frac{Q_c}{V_c}t} + \left(S^{in}_{NH_4^+} + \frac{A_m q_{\max,cat} X_f L_f}{Q_c}\left(\frac{S_{NH_4^+}}{S_{NH_4^+} - K_{S,NH_4^+}}\right) \left[\frac{1}{1+\exp\left(-\frac{F}{RT}\eta\right)}\right]\right)\left(1 - e^{\frac{Q_c}{V_c}t}\right) \tag{26}$$

$$S_{NO_3^-}(t) = S^*_{NO_3^-} e^{\frac{Q_c}{V_c}t} + \left(S^{in}_{NO_3^-} - \frac{A_m q_{\max,cat} X_f L_f}{Q_c} \left(\frac{S_{NH_4^+}}{S_{NH_4^+} - K_{S,NH_4^+}} \right) \left[\frac{1}{1+\exp\left(-\frac{F}{RT}\eta\right)} \right] \right) \left(1 - e^{\frac{Q_c}{V_c}t}\right) \tag{27}$$

$$S_{OH^-}(t) = S^*_{OH^-} e^{\frac{Q_c}{V_c}t} + \left(S^{in}_{OH^-} - \frac{4A_m q_{\max,cat} X_f L_f}{Q_c} \left(\frac{S_{NH_4^+}}{S_{NH_4^+} - K_{S,NH_4^+}} \right) \left[\frac{1}{1+\exp\left(-\frac{F}{RT}\eta\right)} \right] \right) \left(1 - e^{\frac{Q_c}{V_c}t}\right) \tag{28}$$

$$S_M(t) = S^*_M e^{\frac{Q_c}{V_c}t} + \left(S^{in}_M + \frac{N A_m q_{\max,cat} X_f L_f}{Q_c} \left(\frac{S_{NH_4^+}}{S_{NH_4^+} - K_{S,NH_4^+}} \right) \left[\frac{1}{1+\exp\left(-\frac{F}{RT}\eta\right)} \right] \right) \left(1 - e^{\frac{Q_c}{V_c}t}\right) \tag{29}$$

Mass balance for the attached aerobic bioreactor:

$$V_{nb}\frac{dS_{NH_4^+}}{dt} = Q\left(S^{in}_{NH_4^+} - S_{NH_4^+}\right) - r_{nit}V_{nb} \tag{30}$$

$$V_{nb}\frac{dS_{O_2}}{dt} = Q\left(S^{in}_{O_2} - S_{O_2}\right) - r_{nit}V_{nb} \tag{31}$$

$$V_{nb}\frac{dS_{NO_3}}{dt} = Q_c\left(S^{in}_{NO_3} - S_{NO_3}\right) + r_{nit}V_{nb} \tag{32}$$

Where

$$r_{nit} = q_{\max,NH_4^+}\frac{S_{NH_4^+}}{S_{NH_4^+} - K_{S,NH_4^+}}\frac{S_o}{S_o - K_{N,O}}X_n \tag{33}$$

The analytical solution for attached aerobic bioreactor:

$$S_{NH_4^+}(t) = S^*_{NH_4^+} e^{-\frac{Q}{V_{nb}}t} + \left(S^{in}_{NH_4^+} - \frac{q_{\max,NH_4^+}}{Q}\frac{S_{NH_4^+}}{S_{NH_4^+} - K_{S,NH_4^+}} \frac{S_o}{S_o - K_{N,O}}X_n \right)\left[1 - e^{-\frac{Q}{V_{nb}}t}\right] \tag{34}$$

$$S_{O_2}(t) = S^*_{O_2} e^{-\frac{Q}{V_{nb}}t} + \left(S^{in}_{O_2} - \frac{q_{\max,NH_4^+}}{Q}\frac{S_{NH_4^+}}{S_{NH_4^+} - K_{S,NH_4^+}} \frac{S_o}{S_o - K_{N,O}}X_n \right)\left[1 - e^{-\frac{Q}{V_{nb}}t}\right] \tag{35}$$

$$S_{NO_3}(t) = S^*_{NO_3} e^{-\frac{Q}{V_{nb}}t} + \left(S^{in}_{NO_3} + \frac{q_{\max,NH_4^+}}{Q}\frac{S_{NH_4^+}}{S_{NH_4^+} - K_{S,NH_4^+}} \frac{S_o}{S_o - K_{N,O}}X_n \right)\left[1 - e^{-\frac{Q}{V_{nb}}t}\right] \tag{36}$$

Mass balance for the anoxic bioreactor:

$$V_{dn}\frac{dS_{NO_3^-}}{dt} = Q_r\left(S^{in}_{NO_3^-} - S_{NO_3^-}\right) - r_{dn}V_{dn} \tag{37}$$

where

$$r_{dn} = q_{\max,NO_3}\frac{S_{NO_3}}{S_{NO_3} - K_{d,S_{NO_3^-}}}\frac{S_{AC}}{S_{AC} - K_{d,AC}}X_{dn} \tag{38}$$

The analytical solution for anoxic bioreactor:

$$S_{NO_3^-}(t) = S^*_{NO_3^-} e^{-\frac{Q_r}{V_{dn}}t} + \left(S^{in}_{NO_3^-} - \frac{q_{\max,NO_3}}{Q_r}\frac{S_{NO_3}}{S_{NO_3} - K_{d,S_{NO_3^-}}} \frac{S_{AC}}{S_{AC} - K_{d,AC}}X_{dn} \right)\left[1 - e^{-\frac{Q_r}{V_{dn}}t}\right] \tag{39}$$

The combined MFC-AB-NAB system has the following overall mass balance: 1. Transformation of acetate concentration:

$$\frac{dS_{AC}}{dt} = \frac{Q}{V}\left(\frac{S^{in}_{AC} - S_{AC}}{\alpha_{AC,2}}\right) - \left(\frac{Q}{V}\left(S^{in}_{AC}(1-\alpha_{AC,1})\right) - A_m r_{ut,an}\right) - \left(\frac{Q}{V}\left(S^{in}_{AC}(\alpha_{AC,2} - \alpha_{AC,1})\right) - r_{dn}\right) \tag{40}$$

Where

$$r_{ut,an} = q_{\max,m} X_F \varnothing_{E,a}\left(\frac{S_{AC}}{S_{AC} - K_{S,AC}}\right)\left[\frac{1}{1+\exp\left(-\frac{F}{RT}\eta\right)}\right] \tag{41}$$

$$r_{dn} = q_{\max,NO_3}\frac{S_{NO_3}}{S_{NO_3} - K_{d,S_{NO_3^-}}}\frac{S_{AC}}{S_{AC} - K_{d,AC}}X_{dn} \tag{42}$$

The analytical solution are,

$$S_{AC}(t) = S^{*}_{AC} e^{-\frac{Q}{V\alpha_{AC,2}}t} + S^{in}_{AC}(1-\alpha_{AC,2}(1-2\alpha_{AC,1}-\alpha_{AC,2}))\left(1-e^{-\frac{Q}{V\alpha_{AC,2}}t}\right) + \frac{V\alpha_{AC,2}}{Q}\left(A_m q_{\max,m} X_F \varnothing_{E,a}\left(\frac{S_{AC}}{S_{AC}-K_{S,AC}}\right)\left[\frac{1}{1+\exp\left(-\frac{F}{RT}\eta\right)}\right] + q_{\max,NO_3}\frac{S_{NO_3}}{S_{NO_3}-K_{d,S_{NO_5}}}\frac{S_{AC}}{S_{AC}-K_{d,AC}}X_{dn}\right)\left(1-e^{-\frac{Q}{V\alpha_{AC,2}}t}\right) \tag{43}$$

2. Transformation of ammonium concentration:

$$\frac{dS_{NH_4^+}}{dt} = \frac{Q}{V}\left(\frac{S^{in}_{NH_4^+}-S_{NH_4^+}}{\alpha_{NH_4^+,2}}\right) - \left(\frac{Q}{V}(S^{in}_{NH_4^+}(1-\alpha_{NH_4^+,1})) + \frac{A_m}{V}(S_{NH_4^+}+r_{nit,cat})\right) - \left(\frac{Q}{V}(S^{in}_{NH_4^+}(\alpha_{NH_4^+,2}-\alpha_{NH_4^+,1})) + r_{nit}\right) \tag{44}$$

Where

$$r_{nit,cat} = -q_{\max,cat}X_f L_f\left(\frac{S_{NH_4^+}}{S_{NH_4^+}-K_{S,NH_4^+}}\right)\left[\frac{1}{1+\exp\left(-\frac{F}{RT}\eta\right)}\right] \tag{45}$$

The analytical solution are,

$$S_{NH_4^+}(t) = S^{*}_{NH_4^+} e^{-\frac{Q}{V\alpha_{NH_4^+,2}}t} + S^{in}_{NH_4^+}\left(1-\alpha_{NH_4^+,2}(1-\alpha_{NH_4^+,1}+\alpha_{NH_4^+,2}-\alpha_{NH_4^+,1})\right)\left(1-e^{-\frac{Q}{V\alpha_{NH_4^+,2}}t}\right) - \frac{A_m\alpha_{NH_4^+,2}}{Q}\left(N_{MH_4^+} - q_{\max,cat}X_f L_f\left(\frac{S_{NH_4^+}}{S_{NH_4^+}-K_{S,NH_4^+}}\right)\left[\frac{1}{1+\exp\left(-\frac{F}{RT}\eta\right)}\right]\right)\left(1-e^{-\frac{Q}{V\alpha_{NH_4^+,2}}t}\right) - \frac{r_{nit}V\alpha_{NH_4^+,2}}{Q}\left(1-e^{-\frac{Q}{V\alpha_{NH_4^+,2}}t}\right) \tag{46}$$

3. Transformation of nitrate concentration:

$$\frac{dS_{NO_3}}{dt} = \frac{Q}{V}\left(S^{in}_{NO_3}-S_{NO_3}\right) + r_{nit} - r_{den} \tag{47}$$

The analytical solution are,

$$S_{NO_3}(t) = S^{*}_{NO_3}e^{-\frac{Q}{V}t} + \left(S^{in}_{NO_3} + \frac{V}{Q}(r_{nit}-r_{dn})\right)\left(1-e^{-\frac{Q}{V}t}\right) \tag{48}$$

4. Transformation of nitrogen concentration:

$$\frac{dS_{N_2}}{dt} = \frac{Q}{V}\left(S^{in}_{NO_3}-S_{NO_3}\right) \tag{49}$$

The analytical solution are,

$$S_{N_2}(t) = S^{*}_{N_2} + \frac{Q}{V}\left(S^{in}_{NO_3}-S_{NO_3}\right)t \tag{50}$$

4 Results and discussion

The key parameter values employed in the numerical simulations are listed in Table 4.

The concentration decreases for all values of $q_{mxc,an}$ and A_m. Rapid fermentation is a fermentation technique that can achieve high productivity with strains having a high maximum specific growth rate that can be operated. Therefore the value of the maximum specific rate and cross-sectional area of the membrane increases the concentration is also raises. In Figure 2(c) is obtained that it is directly opposite to Figures 2(a) and 2(b). When the value of the half-maximum saturation coefficient for acetate $K_{S,AC}$ is increases the value of acetate also increases for potential.

The value of Nitrate concentration S_{NO_3} increases slightly when the values of V and r_{nit} increases, as shown in Figures 4(b) and 4(c). If the value of nitrification rate and volume is decay, the concentration also decreases. When Figure 4(a) is directly proportional to V and r_{nit}.

From Figures 5(b) and 5(c), infer that a feed flow rate Q and nitrate concentration S_{NO_3} increase when concentration nitrogen increases. Figure 5(a) represented the volume is decay, the concentration is decay.

4.1 Based on the facts and numbers, the following issues are explored in this study effort

The theoretical model created for the combined MFC-OB-ANB system sheds light on the behavior and performance of the hybrid wastewater treatment process. The obtained analytical formulations allow for the prediction of critical system characteristics such as substrate concentrations, nitrogen species dynamics, and energy generation under varied operating situations.

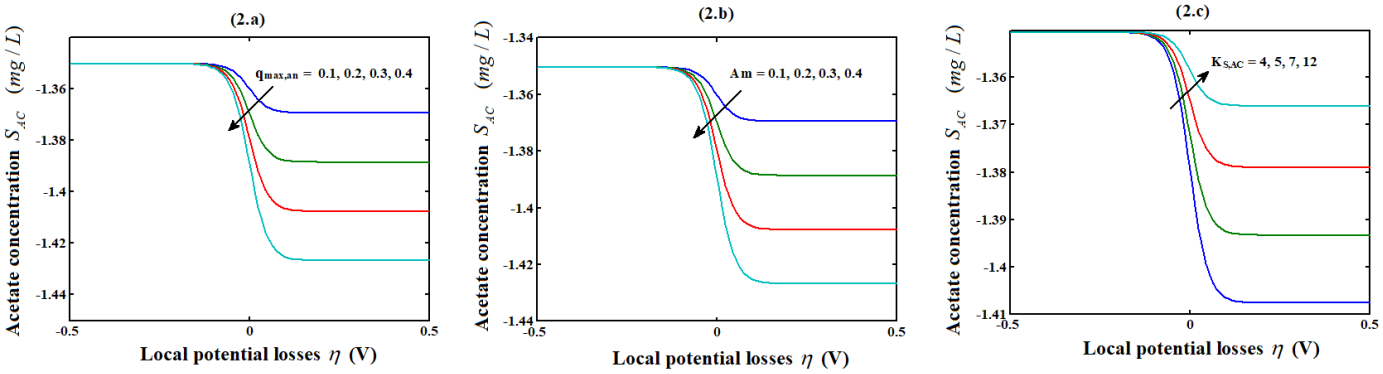

Figure 2. The concentration of acetate SAC versus potential η is shown in Figures 2(a) and 2(b).

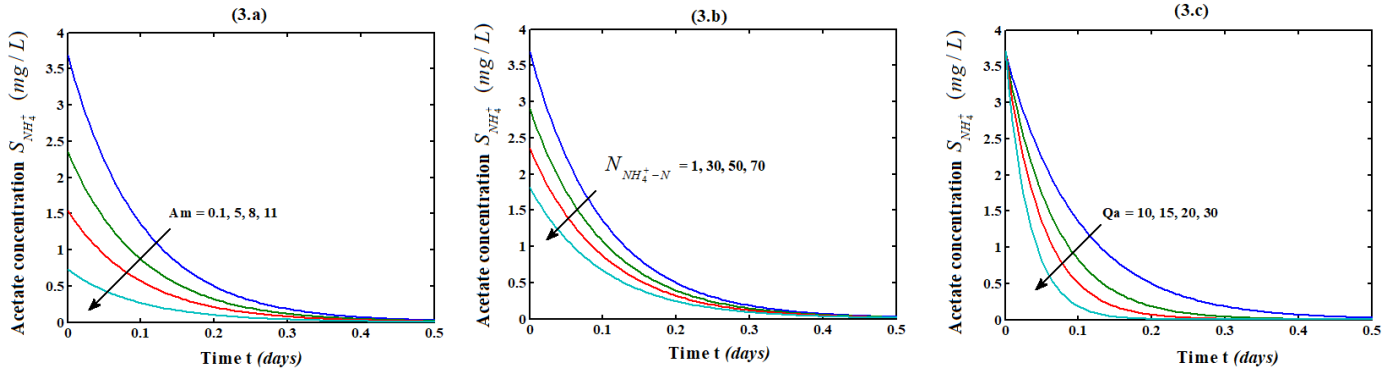

Figure 3. Figures 3(a-c) show that the concentration of acetate falls from its initial value for all parameter values. The concentration also rises when A_m, $N_{NH_4^+-N}$ and Q_a falls.

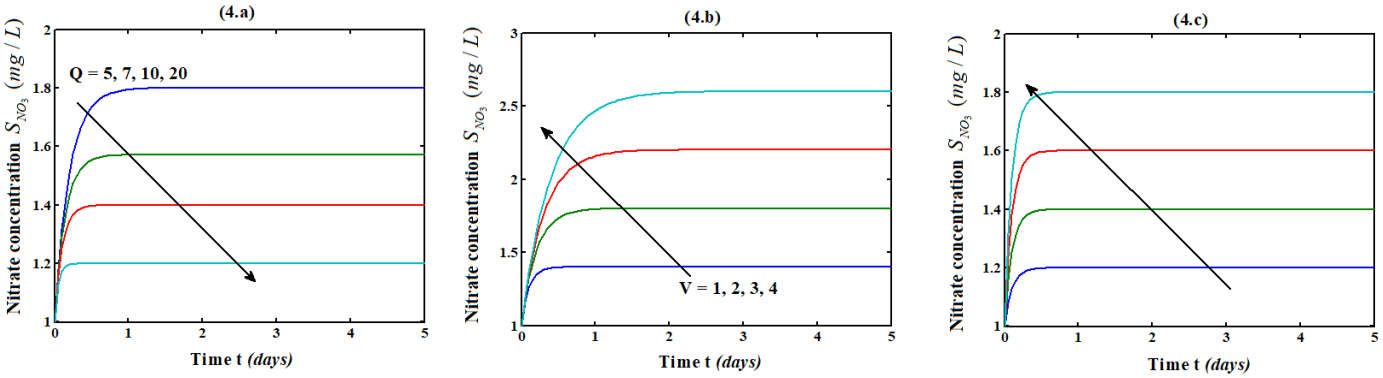

Figure 4. Time versus nitrate concentration for the different values of the parameter and it denotes Eq. (48).

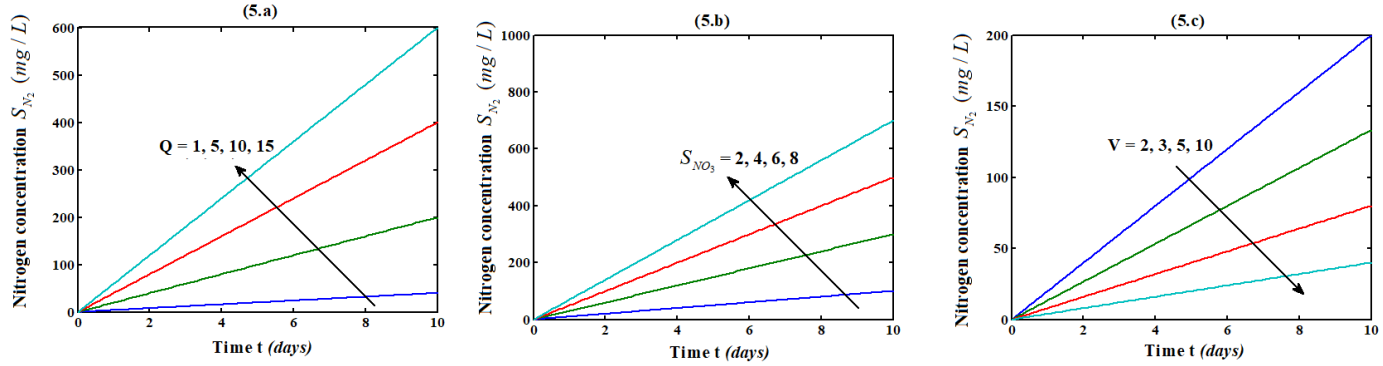

Figure 5. Time versus nitrogen concentration for the different values of the parameter and it denotes Eq. (50).

4.2 Acetate Concentration Dynamics

The model findings show that the concentration of acetate declines gradually throughout the MFC-OB-ANB system as a result of bioelectrochemical oxidation and biological degradation. The simulation shows that increasing biofilm thickness and membrane conductivity results in greater substrate utilization rates, which corresponds to improved electron transfer and microbial activity within the MFC.

4.3 Nitrogen Transformation and Removal

The model accurately depicts the conversion of ammonium to nitrate by nitrification in the oxic bioreactor, followed by denitrification in the anoxic. According to parametric study, dissolved oxygen levels in the OB, nitrate loading rates, and the availability of electron donors (e.g., acetate) for denitrification all have a substantial impact on nitrogen removal efficiency. Maintaining adequate carbon-to-nitrogen ratios has been demonstrated to be crucial for effective nitrogen removal.

4.4 Electricity Generation Performance

The integrated model estimates system voltage and current density based on biofilm features, membrane parameters, and substrate concentration. The results show that improved biofilm conductivity and reduced membrane resistance improve electrical production, giving a dual advantage of energy recovery and wastewater treatment.

Sensitivity analyses show that operational factors including feed flow rates, reactor volumes, and substrate concentrations have a significant impact on overall system performance. The model shows how improving these factors can enhance both pollution removal and energy recovery.

4.5 Integration and System Interactions

The relationship between the MFC, OB, and ANB components is crucial to system stability and performance. The model shows that the sequential arrangement provides progressive treatment, with the MFC reducing organic load, the OB facilitating nitrification, and the ANB completing nitrogen removal via denitrification.

4.6 Limitations and Practical Implications

Although acetate is employed as a simple model substrate, the complex composition of actual slaughterhouse effluent, which includes lipids, proteins, and oils, may have an impact on system efficiency. Predict and optimize system design. Future studies should include experimental validation with actual wastewater to verify the model predictions and enhance system design optimization.

4.7 Impact of Biofilm Thickness

Simulation results indicate that increased biofilm thickness enhances the contact area between electrogenic microbes and substrates, leading to higher current density and improved substrate degradation.

4.8 Membrane Conductivity

A higher membrane conductivity reduces internal resistance and improves electron transfer efficiency. The model shows a proportional increase in system voltage with increasing membrane conductivity.

4.9 Substrate Concentration

Optimal substrate concentrations enhance microbial growth and nitrogen removal efficiency. Excessively high concentrations, however, may inhibit nitrification due to oxygen depletion.

Figures 2–5 demonstrate these effects, with specific parameters labeled. Captions have been expanded to describe parameter values and observed trends.

5 Conclusion

This study develops a comprehensive analytical framework for an integrated MFC–OB–ANB system treating high-strength slaughterhouse wastewater. The derived closed-form solutions elucidate the influence of key operational parameters such as biofilm thickness, membrane conductivity, and substrate concentration on organic matter removal, nitrogen transformation, and electrical energy generation. The results demonstrate that improved biofilm properties and membrane conductivity reduce internal resistance, leading to enhanced current density and system voltage. Efficient integrity between the MFC, oxic, and anoxic reactors enables progressive treatment through organic oxidation, nitrification, and denitrification. Although acetate is used as a representative substrate, the model provides practical insights for optimizing real wastewater treatment systems. The proposed analytical approach serves as a valuable design tool for advancing sustainable bioelectrochemical technologies, with future work focusing on experimental validation using real slaughterhouse effluents.

Data Availability Statement

Data will be made available on request.

Funding

This work was supported without any funding.

Conflicts of Interest

The authors declare no conflicts of interest.

Ethical Approval and Consent to Participate

Not applicable.

References

[1] Bustillo-Lecompte, C. F., & Mehrvar, M. (2015). Slaughterhouse wastewater characteristics, treatment, and management in the meat processing industry: A review on trends and advances. *Journal of environmental management, 161*, 287-302. [Crossref]

[2] Jayashree, C., Tamilarasan, K., Rajkumar, M., Arulazhagan, P., Yogalakshmi, K. N., Srikanth, M., & Banu, J. R. (2016). Treatment of seafood processing wastewater using upflow microbial fuel cell for power generation and identification of bacterial community in anodic biofilm. *Journal of environmental management, 180*, 351-358. [Crossref]

[3] Li, J., & He, Z. (2015). Optimizing the performance of a membrane bio-electrochemical reactor using an anion exchange membrane for wastewater treatment. *Environmental Science: Water Research & Technology, 1*(3), 355-362. [Crossref]

[4] Mittal, G. S. (2006). Treatment of wastewater from abattoirs before land application—a review. *Bioresource technology, 97*(9), 1119-1135. [Crossref]

[5] Bello, Y. O., & Oyedemi, D. T. A. (2009). The impact of abattoir activities and management in residential neighbourhoods: A case study of Ogbomoso, Nigeria. *Journal of Social Sciences, 19*(2), 121-127.

[6] Muhirwa, D., Nhapi, I., Wali, U.G., Banadda, N., Kashaigili, J.J., & Kimwaga, R.J. (2010). Characterization of wastewater from an Abattoir in Rwanda and the impact on downstream water quality. *International Journal of Ecology & Development, 16*, 30-46. [Crossref]

[7] Aniebo, A. O., Wekhe, S. N., & Okoli, I. C. (2009). Abattoir blood waste generation in Rivers State and its environmental implications in the Niger Delta. *Toxicological & Environmental Chemistry, 91*(4), 619-625. [Crossref]

[8] Ruiz, I., Veiga, M. C., De Santiago, P., & Blazquez, R. J. B. T. (1997). Treatment of slaughterhouse wastewater in a UASB reactor and an anaerobic filter. *Bioresource Technology, 60*(3), 251-258. [Crossref]

[9] Rahimi, Y., Torabian, A., Mehrdadi, N., & Shahmoradi, B. (2011). Simultaneous nitrification–denitrification and phosphorus removal in a fixed bed sequencing batch reactor (FBSBR). *Journal of hazardous materials, 185*(2-3), 852-857. [Crossref]

[10] Rajakumar, R., Meenambal, T., Saravanan, P. M., & Ananthanarayanan, P. (2012). Treatment of poultry slaughterhouse wastewater in hybrid upflow anaerobic sludge blanket reactor packed with pleated poly vinyl chloride rings. *Bioresource Technology, 103*(1), 116-122. [Crossref]

[11] Sunder, G. C., & Satyanarayan, S. (2013). Efficient treatment of slaughter house wastewater by anaerobic hybrid reactor packed with special floating media. *International Journal of Chemical and Physical Sciences, 2*, 73-81.

[12] Gerbens-Leenes, P. W., Mekonnen, M. M., & Hoekstra, A. Y. (2013). The water footprint of poultry, pork and beef: A comparative study in different countries and production systems. *Water resources and industry, 1*, 25-36. [Crossref]

[13] Mekonnen, M. M., & Hoekstra, A. Y. (2012). A global assessment of the water footprint of farm animal products. *Ecosystems, 15*(3), 401-415. [Crossref]

[14] Valta, K., Kosanovic, T., Malamis, D., Moustakas, K., & Loizidou, M. (2015). Overview of water usage and wastewater management in the food and beverage industry. *Desalination and Water Treatment, 53*(12), 3335-3347. [Crossref]

[15] Jensen, P. D., Yap, S. D., Boyle-Gotla, A., Janoschka, J., Carney, C., Pidou, M., & Batstone, D. J. (2015). Anaerobic membrane bioreactors enable high rate treatment of slaughterhouse wastewater. *Biochemical Engineering Journal, 97*, 132-141. [Crossref]

[16] Bustillo-Lecompte, C. F., Mehrvar, M., & Quiñones-Bolaños, E. (2014). Cost-effectiveness analysis of TOC removal from slaughterhouse wastewater using combined anaerobic–aerobic and UV/H2O2 processes. *Journal of environmental management, 134*, 145-152. [Crossref]

[17] Pant, D., Van Bogaert, G., Diels, L., & Vanbroekhoven, K. (2010). A review of the substrates used in microbial fuel cells (MFCs) for sustainable energy production. *Bioresource technology, 101*(6), 1533-1543. [Crossref]

[18] ElMekawy, A., Srikanth, S., Bajracharya, S., Hegab, H. M., Nigam, P. S., Singh, A., ... & Pant, D. (2015). Food and agricultural wastes as substrates for bioelectrochemical system (BES): the synchronized recovery of sustainable energy and waste treatment. *Food Research International, 73*, 213-225. [Crossref]

[19] Suganya, S. T., Balaganesan, P., & Rajendran, L. (2019). Mathematical Modeling of Microbial Fuel Cells in Wastewater Treatment-Homotopy Perturbation Method. *International Journal of Recent Technology and Engineering, 8*(4). [Crossref]

[20] Kundu, P., Debsarkar, A., & Mukherjee, S. (2013).

Treatment of slaughter house wastewater in a sequencing batch reactor: performance evaluation and biodegradation kinetics. *BioMed research international*, *2013*(1), 134872. [Crossref]

[21] Mohammed, A. J., & Ismail, Z. Z. (2018). Slaughterhouse wastewater biotreatment associated with bioelectricity generation and nitrogen recovery in hybrid system of microbial fuel cell with aerobic and anoxic bioreactors. *Ecological Engineering*, *125*, 119-130. [Crossref]

[22] Mohammed, H. K., Al-Alawy, A. F., Abbas, T. R., Al-Mosawi, A. I., & Salih, M. H. (2024). Mathematical modeling of osmotic membrane bioreactor process for oily wastewater treatment. *Water Science & Technology*, *90*(7), 2234-2250. [Crossref]

Appendix

A Analytical solution of equation (37) using the HPM method.

Mass balance for the anoxic bioreactor as follows:

$$V_{dn}\frac{dS_{NO_3^-}}{dt} = Q_r\left(S^{in}_{NO_3^-} - S_{NO_3^-}\right) - r_{dn}V_{dn} \quad \text{(A1)}$$

where

$$r_{dn} = q_{\max,NO_3}\frac{S_{NO_3}}{S_{NO_3} - K_{d,S_{NO_3^-}}}\frac{S_{AC}}{S_{AC} - K_{d,AC}}X_{dn} \quad \text{(A2)}$$

Equation (A1) can be written as follows:

$$\frac{dS_{NO_3^-}}{dt} - \frac{Q_r}{V_{dn}}\left(S^{in}_{NO_3^-} - S_{NO_3^-}\right) + r_{dn}V_{dn} = 0 \quad \text{(A3)}$$

The initial conditions are

$$S_{NO_3^-}(t) = S^*_{NO_3^-} \quad \text{(A4)}$$

Homotopy for the above equation (A4) can be constructed as follows:

$$(1-p)\left[\frac{dS_{NO_3^-}}{dt} + \frac{Q_r}{V_{dn}}S_{NO_3^-} - \frac{Q_r}{V_{dn}}S^{in}_{NO_3^-} + r_{dn}\right] + p\left[\frac{dS_{NO_3^-}}{dt} + \frac{Q_r}{V_{dn}}S_{NO_3^-} - \frac{Q_r}{V_{dn}}S^{in}_{NO_3^-} + r_{dn}\right] = 0 \quad \text{(A5)}$$

The approximate solution of the equation (A5) is

$$S_{NO_3^-} = S_{NO_3^-\,0} + pS_{NO_3^-\,1} + p^2S_{NO_3^-\,2} + \ldots \quad \text{(A6)}$$

Substituting Equation (A6) into Equation (A5) and comparing the coefficients of like powers $'p'$

$$\frac{d(S_{NO_3^-\,0} + pNO_3^-{}_1 + \ldots)}{dt} + \frac{Q_r}{V_{dn}}(S_{NO_3^-\,0} + pNO_3^-{}_1 + \ldots) - \frac{Q_r}{V_{dn}}S^{in}_{NO_3^-} + r_{dn} = 0 \quad \text{(A7)}$$

$$p^0 : \frac{dS_{NO_3^-\,0}}{dt} + \frac{Q_r}{V_{dn}}S_{NO_3^-\,0} - \frac{Q_r}{V_{dn}}S^{in}_{NO_3^-} + r_{dn} = 0 \quad \text{(A8)}$$

The initial condition is

$$S_{NO_3^-\,0}(t) = S^*_{NO_3^-} \quad \text{(A9)}$$

Solving equation (A8) with initial condition (A9), yields

$$S_{NO_3^-\,0}(t) = S^*_{NO_3^-}e^{-\frac{Q_r}{V_{dn}}t} + \left(S^{in}_{NO_3^-} - \frac{q_{\max,NO_3}}{Q_r}\frac{S_{NO_3}}{S_{NO_3} - K_{d,S_{NO_3^-}}}\frac{S_{AC}}{S_{AC} - K_{d,AC}}X_{dn}\right)\left(1 - e^{-\frac{Q_r}{V_{dn}}t}\right) \quad \text{(A10)}$$

The solution of the above equation as,

$$S_{NO_3^-}(t) = S_{NO_3^-\,0}(t) \quad \text{(A11)}$$

The solution is,

$$S_{NO_3^-}(t) = S^*_{NO_3^-}e^{-\frac{Q_r}{V_{dn}}t} + \left(S^{in}_{NO_3^-} - \frac{q_{\max,NO_3}}{Q_r}\frac{S_{NO_3}}{S_{NO_3} - K_{d,S_{NO_3^-}}}\frac{S_{AC}}{S_{AC} - K_{d,AC}}X_{dn}\right)\left(1 - e^{-\frac{Q_r}{V_{dn}}t}\right) \quad \text{(A12)}$$

Dr. Muhammad Ijaz Khan received MS and PhD from Quaid-I-Azam University, Islamabad, Pakistan in the year 2016 and 2019 in Applied Mathematics for work in the field of CFD analysis, Flow Behavior and Numerical techniques (AI). Currently working as Assistant Professor in the Department of Mechanical Engineering, Prince Mohammad Bin Fahd University, P. O. Box, 1664, Al-Khobar 31952, Kingdom of Saudi Arabia. Contributed more than 50 research-level papers to many International journals. Research interests include Sensor Networks, Machine Learning, and Cloud computing, Flow Behavior, CFD analysis.